

**RARE EARTH ELEMENT ANALYSIS OF UR CAIS FROM CV3 CHONDRITES BY SRXRF.** P.-T. Genzel<sup>1\*</sup>, B. Bazi<sup>2</sup>, E. De Pauw<sup>2</sup>, B. Vekemans<sup>2</sup>, L. Vincze<sup>2</sup>, J. Garrevoet<sup>3</sup>, M. Lindner<sup>1</sup>, G. Falkenberg<sup>3</sup>, M. A. Ivanova<sup>4</sup>, C. Ma<sup>5</sup>, A. M. Davis<sup>6</sup>, A. N. Krot<sup>7</sup>, F. E. Brenker<sup>1</sup> <sup>1</sup>Goethe University Frankfurt, Institute of Geoscience, Altenhöferallee 1, 60438 Frankfurt am Main, Germany, \*Genzel@em.uni-frankfurt.de; <sup>2</sup>Department of Chemistry, Ghent University, Krijgslaan 281, B-9000 Ghent, Belgium; <sup>3</sup>PETRA III, DESY, Notkestraße 85, 22607 Hamburg, Germany; <sup>4</sup>Vernadsky Institute, Moscow, Russia; <sup>5</sup>California Institute of Technology, Pasadena, USA; <sup>6</sup>University of Chicago, USA; <sup>7</sup>Hawai'i Institute of Geophysics and Planetology, University of Hawai'i at Mānoa, Honolulu, USA.

**Introduction:** Calcium-aluminum-rich inclusions (CAIs) are the oldest known solids formed in the solar system [1], and therefore provide essential constraints on the early stages of the solar system evolution [2]. CAIs are characterized by volatility fractionated bulk rare earth element (REE) patterns indicating important role of evaporation and condensation processes during their formation. Mason and Martin [4] described five distinct REE patterns in CAIs. Group I, III, V and VI CAIs have unfractionated REE patterns and can be distinguished by enrichments/depletions of the relatively volatile elements – Eu and Yb. Group II CAIs have fractionated REE patterns; they are enriched in less refractory REEs and depleted in the most refractory REEs [3]. The group II REE patterns can only arise by fractional condensation in a gaseous reservoir from which the most refractory REEs were removed [4–6]. CAIs that have REE patterns complementary to group II patterns are named ultrarefractory (UR). These CAIs represent the highest temperature fraction which was removed prior group II condensation [4,7–9]. Group II REE patterns occur in 20% of refractory inclusions [10], whereas UR inclusions are rare [7–14]. The mineral carriers of UR REEs have not been determined yet. Several CAIs with UR REE patterns are composed of very refractory minerals including Zr,Sc-rich oxides, Zr,Sc,Y-rich pyroxenes, and Y,Ti-rich perovskite [10,13,14]. We have recently characterized the mineralogy, petrography, and oxygen-isotope compositions of ~20 CAIs containing abundant Zr- and Sc-rich minerals in several carbonaceous chondrite groups (CR, CM, CO, CV, CH) and suggested that these minerals could represent the carriers of UR REE patterns [19]. To confirm the UR character of the CAIs containing Zr- and Sc-rich minerals and determine mineral carriers of UR patterns, we measured REE patterns in three of these CAIs, *Al-2*, *33E-21*, and *2N-24*, with synchrotron radiation X-ray fluorescence spectrometry (SRXRF)

**Mineralogy and Petrography:** The detailed mineralogy, petrography and O-isotope compositions of CAIs *Al-2*, *33E-1* and *3N-24* from the CV3 chondrites Allende, Efremovka, and Northwest Africa (NWA) 3118, respectively, have been previously reported by [2,15]. *Al-2* is a forsterite-bearing Type B (FoB) CAI that contains a relict CAI, ~100 µm in size, consisting

of irregularly-shaped fine-grained objects composed of closely intergrown spinel, perovskite, and eringaite embedded in davisite [2]. *33E* is a compound object composed of an amoeboid olivine aggregate (AOA), a fluffy Type A (FTA) CAI and the UR CAI *33E-1* [2,15]. *33E-1* has a nodular-like texture; it consists of Y-rich perovskite, Zr,Sc,Y-rich pyroxenes (Al,Ti-diopside, Sc-rich pyroxene), Zr,Sc,Y-rich oxides (tazheranite), spinel, and gehlenite [15]. Individual nodules are surrounded by Wark-Lovering rims composed of spinel, Sc-bearing Al-diopside, and forsterite [2,15]. The compound FoB CAI *3N* is composed of 25 CAIs with different textural types, including Compact Type A, Type B, Type C and UR [2,15]. The UR CAI *3N-34* consists of Zr,Sc-rich oxides (tazheranite) that contain small inclusions of perovskite, and are surrounded by Zr,Sc-rich Al,Ti-diopside containing small inclusions of spinel [2,15,16].

**Analytical Methods:** The compositions of the CAI minerals were analyzed with the scanning electron microscope JOEL JMS 6400, equipped with an INCA energy dispersive X-ray (EDX) spectrometer at the Institute of Geoscience, Goethe University Frankfurt, Germany. Operating conditions were 15kV accelerating voltage, 24 µA beam current, and a measurement time of 100s for each EDX point measurement. An energy calibration on copper was performed prior to EDX analysis. Rare earth element concentrations of the individual minerals (Zr,Sc,Y-rich oxides, Zr,Sc-rich pyroxene, Y-rich perovskite, pyroxene, and spinel) in the CAIs *Al-2*, *33E-1*, and *3N-24* were measured with the energy dispersive (ED) set up at the Hard X-ray Micro/Nano-Probe beamline P06 at the Deutsches Elektronen-Synchrotron (DESY) in Hamburg, Germany. For SRXRF the samples were measured in a position characterized by a 13 µm (H) x 7 µm (V) beam size at an excitation energy of 69.16 keV. The used reference materials for REE quantification are NIST SRM 612 and ATHO-G, typical live time was 1000 s.

**Results:** The SRXRF measurements yield REE patterns with a strong UR trends for all measured phases of each individual CAI (Fig. 1). HREEs are strongly enriched over LREEs with abundance values up to  $2.6 \times 10^5$  CI (nwa3118 46). Ce is the most depleted REE in all patterns. Ho is the most enriched HREE in all

patterns of *Al-2* and *33E-1*. In *3N-24* patterns, Er (point measurements nwa3118 40, nwa3118 43, and nwa318 45) and Lu (nwa3118 42, and nwa3118 46) are the most enriched HREEs. All patterns show strong depletion in Yb. All minerals display similar curve shapes, only differing in elemental abundances of the individual CAIs. No phase shows significant different patterns compared to other phases. Even the most refractory minerals with high Zr and Sc contents, eringaite and tazheranite, do not display significant different REE patterns compared to the less refractory minerals within the same CAI. Therefore, it was not possible to identify a single carrier phase of UR REE patterns. It became evident that all phases in CAIs enriched in Zr,Sc,Y-rich CAIs have UR REE patterns.

**Discussion:** SRXRF studies confirm the ultrarefractory character of CAIs containing abundant Zr- and Sc-rich minerals, previously assumed to be ultrarefractory on their bulk chemical compositions being highly enriched in zirconium, scandium and yttrium. The REE patterns of *Al-2*, *33E-1* and *3N-24* are strongly fractionated with high enrichments of the HREEs over the LREEs. In each CAI, the different measured minerals display very similar patterns showing no correlation between REE patterns and host phases. Thus, no specific carrier phase of UR patterns has been identified in this study. The lack of correlation between trace element patterns and host phases was previously observed by studies of the Efremovka UR CAI *101.1* by [12] and of Ningqiang (C3 ungrouped chondrite) inclusions by [17], where all phases showed similar REE patterns, suggesting formation from the same reservoir with UR REE signature [12]. We suggest that all constitutes of the UR CAIs *Al-2*, *33E-1* and *3N-24* could have originated in the solar nebula region(s), possibly by condensation.

**Conclusion:** The SRXRF studies of the UR CAIs *Al-2*, *33E-1* and *3N-24* show no significant variation between the observed UR patterns and the host phases. The previous assumption based on the CAI constitutes (Zr,Sc,Y-rich minerals) that these CAIs represent ultrarefractory inclusion has been confirmed by their REE patterns. Nevertheless, it was not possible to identify unique carrier phases of UR patterns, which were presumed to be Zr,Sc,Y-rich minerals. We infer all constitutes of a single UR CAIs originate in the same solar nebula region possibly by condensation.

**References:** [1] Connelly M. (2012) *Science* 338:651–655. [2] Krot, A. N. et al. (2018) *Lunar Planet. Sci.* 49:2083. [3] MacPherson G.J. (2014) *Treatise Geochem.* 2:139–179. [4] Mason B. and Martin P. M. (1977) *Smithson. Contrib. Earth Sci.* 19:84–95. [5] Boynton W. V. *Geochim. Cosmochim. Ac.* 39:569–584. [6] Davis A. M. and Grossman

L. (1979) *Geochim. Cosmochim. Acta* 43:1611–1632. [7] Noonan A. F. et al. (1977) *Meteoritics* 12:332. [8] Palme F. (1982) *Earth Planet. Sci. Lett.* 61:1–12. [9] Davis A.M. (1984) *Meteoritics* 19:214. [10] Davis A.M. (1991) *Meteoritics* 26:330. [11] Simon S.B. et al. (1996) *Meteorit. Planet. Sci.* 31:106–115. [12] El Goresy A. et al. (2002) *Geochim. Cosmochim. Acta* 66:1459–1491. [13] Hiyagon H. et al. (2003) *Lunar Planet. Sci.* 34:1552. [14] Uchiyama K. et al. (2008) *Lunar Planet. Sci.* 39:1519. [15] Ivanova M. et al. (2012) *Meteorit. Planet. Sci.* 47:2107–2127. [16] Ivanova M. et al. (2015) *Meteorit. Planet. Sci.* 50:1512–1528. [17] Hiyagon H. et al. (2011) *Geochim. Cosmochim. Acta* 75:3358–3384. [18] Lodders K. et al. (2010) *Astrophys. Space* 379–471.

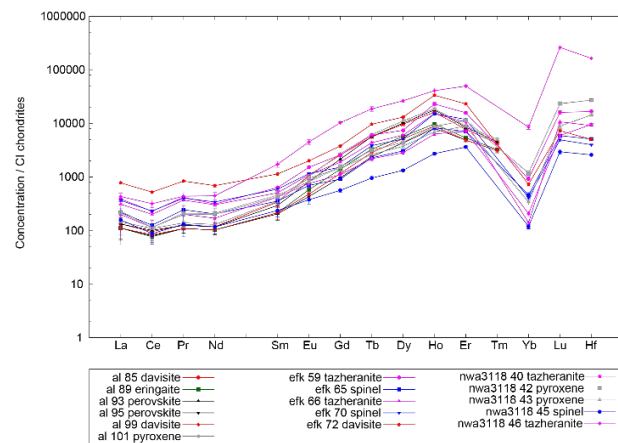


**Fig.1.** REE patterns of *Al-2*, *33E-1* and *3N-24*. The concentrations are CI normalized after Lodders et al. [18]. The point measurements of the SRXRF measurement with the associated minerals determined by EDX are shown in the legend. Patterns of davisite are red, eringaite green, perovskite black, pyroxene grey, spinel blue and tazheranite pink.